Journal of Molecular Catalysis A: Chemical 335 (2011) 71–81

Contents lists available at ScienceDirect

Journal of Molecular Catalysis A: Chemical

journal homepage: www.elsevier.com/locate/molcata

A study of furfural decarbonylation on K-doped Pd/Al_2O_3 catalysts

Wei Zhang[a,b], Yulei Zhu[a,c,*], Shasha Niu[a,b], Yongwang Li[a,c]

[a] State Key Laboratory of Coal Conversion, Institute of Coal Chemistry, Chinese Academy of Sciences, P.O. Box 165, Taiyuan 030001, PR China
[b] Graduate University of the Chinese Academy of Sciences, Beijing 100039, PR China
[c] Synfuels China Co. Ltd, Taiyuan 030001, PR China

ARTICLE INFO

Article history:
Received 15 September 2010
Received in revised form
10 November 2010
Accepted 14 November 2010
Available online 21 November 2010

Keywords:
Decarbonylation
Furfural
Furan
Pd/Al_2O_3 catalysts
2-Methylfuran

ABSTRACT

Vapor-phase decarbonylation of furfural to furan was performed on K-doped Pd/Al_2O_3 catalysts in a fixed-bed reactor. A series of K-doped catalysts were prepared by impregnation method with various potassium salt precursors and different potassium content. The catalyst evaluation results revealed that the doping of K not only promoted the furfural decarbonylation, but also suppressed the hydrogenation side reaction. Among the investigated catalysts, $Pd–K_2CO_3/Al_2O_3$ (K% = 8 wt.%) presented the best performance and achieved the furan yields up to 99.5% at 260 °C. The selectivity of 2-methylfuran would approach zero at high K content (K% > 4 wt.%). Furthermore, the catalysts were characterized by BET, SEM, ICP, H_2-TPR, H_2-TPD, H_2-chemisorption, CO-FTIR, furfural-TPSR, and furfural-FTIR experiments. It was shown that the dopant phase had a remarkable effect on the precursor Pd^{2+} and the reduced Pd metal particles. Furfural-TPSR and furfural-FTIR exhibited that K-doped catalysts enhanced the furfural adsorption and promoted the decarbonylation reaction, which was due to the different adsorption mode and intensity of furfural on K-doped and undoped samples. Besides, the decrease of C–O adsorption of furfural (η_2(C,O)-furfural) by K doping is the main reason for suppressing the furfural hydrogenation.

© 2010 Elsevier B.V. All rights reserved.

1. Introduction

Transformation of non-food biomass to chemicals is an important sustainability issue and has attracted much attention in recent years [1]. Furfural, as an important chemical readily accessible from biomass, appears to be the only unsaturated large-volume organic chemical prepared from carbohydrate resources and is a key derivative for the production of non-petroleum-derived chemicals [2]. One important chemical coming from furfural is furan [1–5], which is a useful intermediate and employed primarily in the synthesis of tetrahydrofuran. Both vapor [3] and liquid phase [5] decarbonylation of furfural can produce furan, but vapor phase decarbonylation is usually preferred for its simple operation, easy separation, handling and recycling of catalysts.

Some metal oxides such as iron, zinc, manganese, molybdenum, chromium oxides, or their mixtures [6–8] and noble metals such as Pd, Pt, Rh used as supported form [9,10] are employed as the catalysts for decarbonylation of furfural to furan. The main drawback of the non-noble oxide catalysts is the drastic operating conditions, which may bring about a significant breakdown of furan and the formation of heavy products resulting in deactivation of the catalysts [6,7]. In contrast to the non-noble catalyst systems, the supported noble metal catalysts exhibit high conversion and yield at much lower temperatures [9]. For the supported Pd catalysts, the most effective and widely used supports for the decarbonylation reaction are active carbon and alumina [11]. Furthermore, some additives, such as nickel, rhodium, ruthenium, alkali and alkaline-earth metals, are added to modify the properties of supports and interact with the metal, among which alkali metals are the best promoters to the reaction [12].

It should be noted that the vapor-phase decarbonylation must be carried out in the presence of hydrogen as carrier gas, which has the function of prolonging the catalysts life [9]. However, the life expectancy of the catalysts is still not long enough for industrial application and the reason may be the lower ratio of H_2 to furfural. Most of the references reported that the molar ratio of H_2 to furfural should not be higher than 2, and the best range is from 0.5 to 1 [9]. Srivastava and Guha [13] reported that the main reason for catalysts deactivation is the formation of coke, and explained that the rate of deactivation is presumed to be controlled by the reaction between two adsorbed furfural to form coke precursor followed by coking. Therefore, the ratio of H_2 to furfural is chosen as 20 in this study, which obviously prolongs the catalysts life and shows no sign of deactivation through hundreds of hours. However, the high content of hydrogen existed in the reactant gases can produce significant quantities of C=O hydrogenation

* Corresponding author at: State Key Laboratory of Coal Conversion, Institute of Coal Chemistry, Chinese Academy of Sciences, P.O. Box 165, Taiyuan 030001, PR China. Tel.: +86 351 7117097; fax: +86 351 7560668.
E-mail address: zhuyulei@sxicc.ac.cn (Y. Zhu).

1381-1169/$ – see front matter © 2010 Elsevier B.V. All rights reserved.
doi:10.1016/j.molcata.2010.11.016

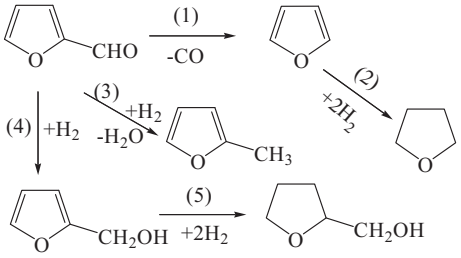

Fig. 1. Main reactions existed in furfural decarbonylation.

by-products. The main reactions occur in furfural decarbonylation as shown in Fig. 1, including the decarbonylation of furfural to furan (1), hydrogenation of furan to tetrahydrofuran (2), hydrogenation of furfural to 2-methylfuran (3), furfuryl alcohol (4) and tetrahydrofurfuryl alcohol (5). Accordingly, this complication may arise during separation and product purification. As the final product, tetrahydrofuran can be obtained by furan hydrogenating without separating it from the gaseous products of furfural decarbonylation. Among these products, furfuryl alcohol (T_{boil} = 171 °C) and tetrahydrofurfuryl alcohol (T_{boil} = 178 °C) can be easily separated with furan (T_{boil} = 32 °C) and tetrahydrofuran (T_{boil} = 66 °C). However, 2-methylfuran (T_{boil} = 63.5 °C) has a similar boiling point with tetrahydrofuran, which makes it very difficult for separation. Therefore, it should be considered to reduce the by-products of furfural hydrogenation, especially 2-methylfuran. Potassium promoter can be employed to inhibit the hydrogenation function of catalyst, which has been proved to be effective in the iron catalysts for F-T synthesis [14]. So, it is expected that the addition of potassium promoter can suppress the hydrogenation of Pd/Al_2O_3.

To the best of our knowledge, few reports have studied the vapor decarbonylation of furfural on high H_2/furfural ratio (≥20) and the low reaction temperature range (180–260 °C). Besides, the effect of K promoter on Pd catalysts is not systematically investigated in this reaction. Therefore, the objectives of this work are to achieve high yield of furan at low temperature and study the effect of K promoter. More specifically, this work is devoted: (a) to choose the best K precursor; (b) to study the effect of K content; (c) to investigate the role of K on the catalytic behavior of Pd catalyst. The structure and redox properties of $Pd–K/Al_2O_3$ catalysts are characterized by BET, ICP, H_2-TPR, CO-FTIR, H_2 chemisorption, H_2-TPD, SEM, furfural-TPSR, and furfural-FTIR aimed at defining the interaction between metals and adsorption mode of furfural.

2. Experimental

2.1. Catalyst preparation

γ-Al_2O_3, obtained from the Aluminum Co., Ltd, of China (surface area = 233 m^2/g, 20–40 mesh), was used as support. 1 wt.% Pd/γ-Al_2O catalyst was prepared by incipient wetness impregnation. Firstly, $Pd(NO_3)_2$ solution was impregnated to the Al_2O_3 at ambient temperature for 5 h. After that, the sample was dried overnight at 120 °C and then calcined at 450 °C for 6 h. The 1 wt.% Pd/Al_2O_3 is referred to as PA.

Five different 1–1 wt.% for $Pd–K/Al_2O_3$ catalysts were prepared using different potassium salts (K_2CO_3, KOH, KCl, KNO_3, CH_3COOK) as K precursors. Firstly, potassium solutions were impregnated to the Al_2O_3 for 0.5 h before $Pd(NO_3)_2$ solutions were added in. The subsequent drying and calcination procedures were the same as those of the Pd/Al_2O_3. The catalysts are designed as PA–X, with X denoting the different potassium salts. For example, PA–K_2CO_3 designates the K in $Pd–K/Al_2O_3$ catalyst coming from K_2CO_3.

Different content of potassium was doped to the Al_2O_3 using K_2CO_3 as K precursor and the loading range was from 0.75 to 10 wt.%. The preparation procedures of the catalysts were the same as PA–K_2CO_3. These catalysts are labeled as PA–K(x), while x is denoting the K content. The PA–K(1%) means the content of K in the $Pd–K/Al_2O_3$ catalyst is 1 wt.%.

2.2. Catalysts characterization

The surface area and textural propertied of the fresh catalysts were measured by nitrogen physical adsorption at 77.4 K with ASAP 2420 (Micromeritics, USA). The catalyst samples were degassed at 350 °C for 9 h prior to the measurement.

The morphologies of as-prepared samples were investigated by SEM (Quanta 400F). From this technique the surface morphology of the catalysts can be obtained.

ICP optical emission spectroscopy (Optima 2100DV, PerkinElmer) was used to analyze the chemical composition of the catalysts. From this technique the exact composition of metal components can be obtained.

The temperature-programmed reduction of H_2 (H_2-TPR) was performed in a conventional apparatus (Micromeritics Auto Chem. 2920, USA) with a thermal conductivity detector. The catalysts were heated at a linear rate of 10 °C/min from room temperature or −80 °C to 500 °C in a 5% H_2/Ar mixture (mol/mol) flowing at 50 ml/min. During the TPR, a liquid nitrogen/isopropanol trap was used to condense the product water in the effluent.

H_2 chemisorption was performed in a surface area and porosity analyzer (Micromeritics. ASAP 2020, USA). The method was used to determine the dispersion of Pd and the amount of hydrogen chemisorption. Prior to measurements, the catalysts were degassed for several hours, and then reduced in hydrogen at 350 °C for 2 h followed by degassing at the same temperature for 2 h. After cooling under vacuum to the adsorption temperature, the total H_2 uptake (adsorption at the Pd surface and adsorption in the bulk) was measured. Next, inert gas (He) was used to remove the physisorbed hydrogen, and then the amount of chemisorbed hydrogen was obtained.

The temperature-programmed desorption of H_2 (H_2-TPD) was performed in the same apparatus as H_2-TPR. The catalysts were first reduced by H_2 at 350 °C for 2 h, and then purged with Ar at the same temperature for 30 min followed by cooling down to 50 °C. After adsorption of H_2 at 50 °C for 30 min, the sample was purged with Ar again in order to remove the weakly adsorbed species until the baseline leveled off. Following this, the H_2 desorption was being carried out from 50 °C to 800 °C at a linear rate of 10 °C/min.

CO-FTIR spectra were collected using an infrared spectrometer (VERTEX70, Bruker, Germany), equipped with KBr optics which works at the liquid nitrogen temperature. The infrared cell with ZnSe windows was connected to a gas-feed system with a set of stainless steel gas lines, which allowed the in situ measurement for the adsorption of CO. Before measurements, the catalysts were reduced in situ at 350 °C for 2 h. After the reduction procedure, the system was cooled to 20 °C and the CO-FTIR spectra were recorded.

The temperature-programmed surface reaction of furfural (furfural-TPSR) was performed in a self-made reactor connected to an on-line mass spectrometer (OmniStar TM). Firstly, the catalysts were reduced by H_2 at 350 °C for 2 h, and then purged with He at the same temperature for 30 min and cooled to 40 °C overnight in order to diminish the effect of H_2. Next, the absorption of furfural was in situ performed at 40 °C by a stream of furfural (diluted with carried gas He) for 1.5 h. After the absorption, the catalysts were purged with He for removing the physically adsorbed furfural at 40 °C until the values of m/e became constant. The TPSR experiments were performed with a heating rate of 10 °C/min in a flow

Table 1
Surface area and pore structure of the catalysts with doping different K salts.

Catalyst	Surface area (m^2/g)	Pore volume (cm^3/g)	Average pore size (nm)
γ-Al_2O_3	196.6	0.619	9.07
PA	191.12	0.611	9.36
PA–K_2CO_3	184.34	0.605	9.73
PA–KOH	182.70	0.602	9.59
PA–KCl	178.48	0.601	9.73
PA–KNO_3	176.42	0.605	9.92
PA–KAc	193.11	0.610	9.26

of He stream, and the desorbing products were monitored with the online MS.

Furfural-FTIR spectra were collected with a VERTEX70 spectrometer cooled by liquid nitrogen. A vacuum pump was used to pull the furfural vapor through the chamber for in situ FTIR measurements. Before the measurements, the catalysts were reduced in situ at 350 °C for 2 h. After the reduction procedure, the system was cooled to 30 °C and the Furfural-FTIR spectra were recorded. Then, the temperature was increased from 30 °C to 200 °C so as to further evaluate the strength of adsorption and the capability of furfural decarbonylation.

2.3. Catalytic test

The activity tests for catalytic decarbonylation of furfural over the Pd catalysts were performed in a fixed bed reactor under atmospheric pressure. Prior to the reactions, the catalysts (20–40 mesh, 2.5 g) were in situ reduced in a stream of pure H_2 (150 ml/min) at 200 °C for 12 h. After reduction, furfural and H_2 were introduced into the fixed-bed reactor through a saturator, and the downstream flow lines of the saturator were maintained at 140 °C to prevent condensation of vaporized furfural. The decarbonylation activity tests were performed in the temperature range of 180–260 °C, and the liquid products were obtained by a cold trap filled with water. The reactants and the products were analyzed using a GC-950 gas-chromatograph (GC) equipped with flame ionization detector and a capillary column (OV-101).

3. Results

3.1. Catalysts characterization

3.1.1. Morphology and sample composition (BET, ICP, SEM)

The BET surface area, pore volume and average pore size are summarized in Tables 1 and 2.

Table 1 shows a decrease in surface area and pore volume, as well as an increase in average pore size compared with the support in all the catalysts, which may be due to pore blocking. However, the deposit of Pd and different K salt precursors on γ-Al_2O_3 support has no obvious effects on the surface areas changes. That is, the variations in the surface areas of these catalysts can be considered as a negligible factor for the different catalytic activities of furfural decarbonylation, which will be shown in catalytic performance.

Table 2 displays the morphology and sample composition of Pd catalysts with different K content. With the increase of K loading, the surface area and pore volume are decreased monotonous due to pore blocking. The ICP results indicate that the content of Pd does not change too much upon different K content. However, there is a more rapid decline in K content at high K loading.

Fig. 2 exhibits that the outer surface of the catalysts with higher K content (such as PA–K(8%)) is covered by elongated crystals other than the support that are not observable before doping K or lower K content, which is constituted mainly by alkaline metal carbonates as found by EDS analysis [15].

3.1.2. H_2-TPR

TPR experiments can be used to investigate the reducibility of the Pd^{2+} species loaded on a given support. By analyzing the TPR results of the undoped and doped samples, it is possible to determine whether dopants have interacted with the supported Pd^{2+} precursor before or during reduction [15].

The TPR profiles of PA and the whole set of K-doped samples (PA–K(x)) are shown in Fig. 3, in which (a) and (b) represent that the experiment starts from room temperature and far below ambient temperature (−80 °C), respectively. As displayed in Fig. 3a, the catalysts with low K content or without K can be easily reduced from the first beginning, and a negative peak at about 72.5 °C is appeared on PA catalyst, which may be due to β-palladium hydride desorption [16]. In hydrogen atmosphere, PdO is reduced easily at ambient temperature to Pd metal, further interacts with hydrogen resulting in the formation of PdH_x species. This progress appears to have occurred during the passage of reducing gas prior to the start of the temperature program, and then the PdH_x will be decomposed with the increase of temperature [17]. However, the desorption peak is weak or disappeared with the increase of K content and the reason may be the presence of electropositive alkali atoms in the vicinity Pd sites, which exhibits higher electron-donating properties and causes the Pd–H bond strength weaker.

In order to avoid the partial reduction of Pd^{2+} species during stabilization of the baseline, a low-temperature H_2-TPR analysis seems to be a feasible approach (Fig. 3b). As displayed in Fig. 3b, the reduction curve of the PA catalyst shows no negative peak and the high temperature peak has a little shift to low temperature compared with Fig. 3a. The PA sample shows a single reduction peak starting at 25 °C and terminating at 75 °C (the peak at 50 °C). With the incorporation of small amounts of K, an additional peak appears at about 155 °C. Further increasing the K content, the intensity of the high temperature peak is progressive increased, and the peak systematically shifts to lower temperature. For example, the peak undergoes a shift from the value 122 °C in PA–K(4%) to 107 °C in PA–K(8%). Contrarily, with the increase of K loading in the catalyst, the intensity of low temperature peak is decreased to a great extent, and the peak simultaneous shifts to higher temperature. The

Table 2
Characterization of the catalysts with doping different K content: surface area and pore structure, chemical composition, hydrogen chemisorption and metallic dispersion.

Catalyst	Surface area (m^2/g)	Pore volume (cm^3/g)	Average pore size (nm)	Pd (wt.%)	K (wt.%)	Δ (K/wt.%)[a]	H_2 chemisorption (mmol/g)	Pd dispersion[b] (%)
PA	191.12	0.611	9.36	0.86	0	0	0.00988	21.0233
PA–K (0.75%)	191.82	0.609	9.42	0.80	0.66	0.09	0.00948	20.1753
PA–K (2%)	186.46	0.590	9.23	0.89	1.76	0.24	0.01398	29.7578
PA–K (4%)	179.77	0.563	9.03	0.89	3.67	0.33	0.01644	34.9739
PA–K (6%)	166.28	0.520	9.09	0.92	4.93	1.07	0.01811	38.5475
PA–K (8%)	146.62	0.497	9.02	0.87	6.64	1.36	0.01567	33.3399
PA–K (10%)	140.10	0.456	9.40	0.88	8.43	1.57	0.02379	50.6189

[a] The difference value of calculated value and true value determined by ICP.
[b] Pd dispersion determined from H_2-chemisorption.

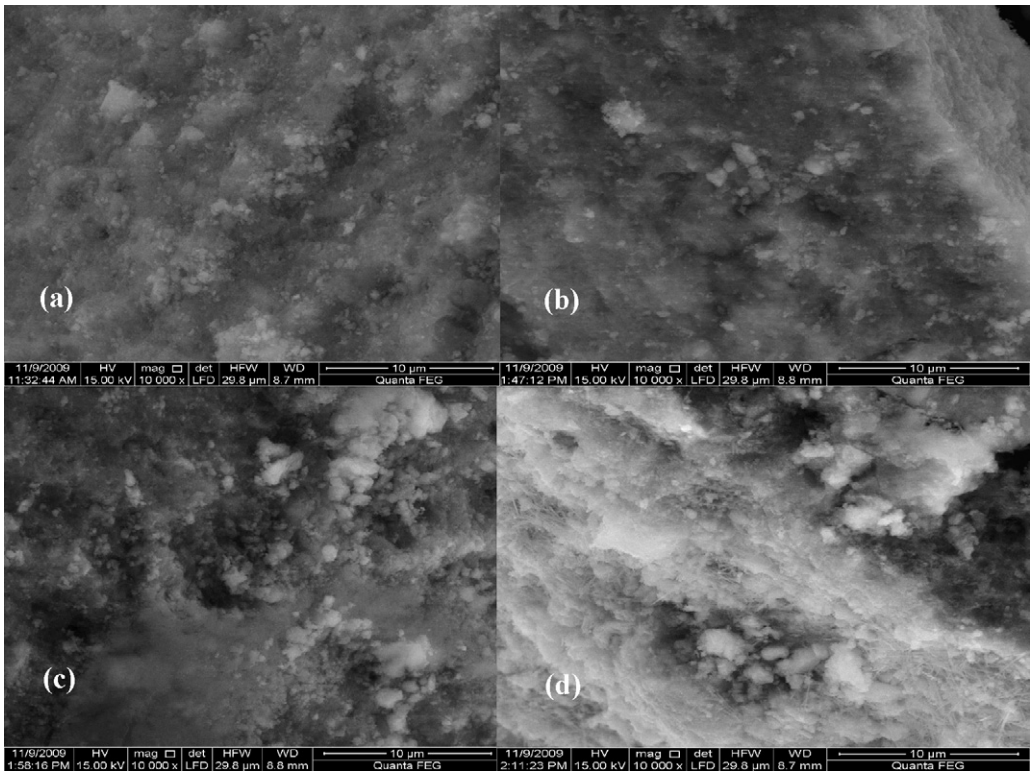

Fig. 2. SEM images of the surface of catalyst particles (10 μm): (a) PA, (b) PA–K(2%), (c) PA–K(4%), and (d) PA–K(8%).

results indicate that more and more K^+ will be interacted with Pd^{2+} with the increase of K content, which lead to change the reduction temperature. The behavior up to K/Pd = 4 reflects a strong chemical interaction between K^+ and Pd^{2+} species, which may eventually lead to the formation of a mixed compound (KPdO) even at low K content [15].

3.1.3. H_2-TPD and H_2 chemisorption

The H_2-TPR results exhibit that the dopant phase has already interacted with the precursor Pd^{2+} phase. One of the questions is whether the interaction between K and Pd is still holding on the reduced Pd metal particles, so the experiments of H_2-TPD and H_2 chemisorption were carried out on the reduced Pd particles. The results are shown in Fig. 4 and Table 2.

It is observed from Fig. 4 that hydrogen desorbs from the samples exhibiting three peaks centered. The low-temperature peak is due to hydrogen chemisorption on the surface of Pd crystallites, whereas the high-temperature feature can be attributed to spillover hydrogen associated with the support. The medium-temperature peak has been assigned to hydrogen adsorbed on the sites located at the periphery of Pd crystallites, which are contacted with the support [18]. K addition does not appreciably affect the position of the low-temperature peak (at ca. 85 °C). However, the high-temperature peaks (at ca. 480 °C) decrease in intensity and have a little shift to higher temperature in the presence of K. The reason is that K can induce the dehydroxylation of support, which is known to suppress the hydrogen spillover. Regarding the medium-temperature peaks (at ca. 300 °C), they decrease in intensity or overlap with the high-temperature peaks except the catalyst PA—(6%). This implies that the adsorption strength of the corresponding sites toward hydrogen decreases in the presence of K. However, it is interesting to see that these effects do not decrease the quantity of adsorbed hydrogen. On the contrary, the adsorbed hydrogen is increased as indicated by the results of H_2-chemisorption (Table 2), which may be due to the higher dispersion of Pd metal particles. From the results, we may draw the conclusion that K has interacted with the reduced Pd. Then, CO-FTIR was carried out as a complement experiment to further investigate this interaction.

3.1.4. CO-FTIR

FTIR spectroscopy of adsorbed CO is a method for the characterization of the electronic states of supported metals. According to the σ–π binding mode reported by Davydov [19], the carbon monoxide molecules adsorbing on metal atoms or ions interact with their valence d-elections and the frequency of the stretching vibration of C–O bond of the surface M–CO complex depends directly on the effective charge of the adsorption.

The FTIR spectra of CO adsorbed at 20 °C on Pd/Al_2O_3 and the K-doped Pd/Al_2O_3 samples are displayed in Fig. 5a–g. The spectra of the catalysts show three main peaks from high-frequency region (2000–2100 cm^{-1}) to low-frequency (1800–2000 cm^{-1}). The interpretation of CO absorption bands on supported palladium catalysts is well defined in the literature [19,20]. The signals in the range 1850–1980 and 2050–2100 cm^{-1} are attributed to bridge Pd–CO–Pd and linear Pd–CO species. Moreover, the two bridged adsorption bands, from high-frequency to low-frequency, can be attributed to the compressed and isolated bridged carbonyls [21] or the twofold bridged carbonyls on Pd(1 0 0) and Pd(1 1 1) faces [22], respectively. As shown in Fig. 5, the progressive increase of K content causes a gradual modification of the CO spectra, suggesting that the dopant has interacted with the reduced Pd metal particles.

As implied by the CO-FTIR characterization, the changes in CO spectra with the increase of K loading can be summarized in three main phenomena. (1) With the increase of K content, the intensity of adsorption band is increased, especially for the catalyst PA–K(8%), which shows the highest CO adsorption band. (2) The bands I and II are progressive decrease of the intensity with respect to the PA catalyst, and a simultaneous increase of band III. At the 8% K loadings, the spectra are dominated by the last band, which is

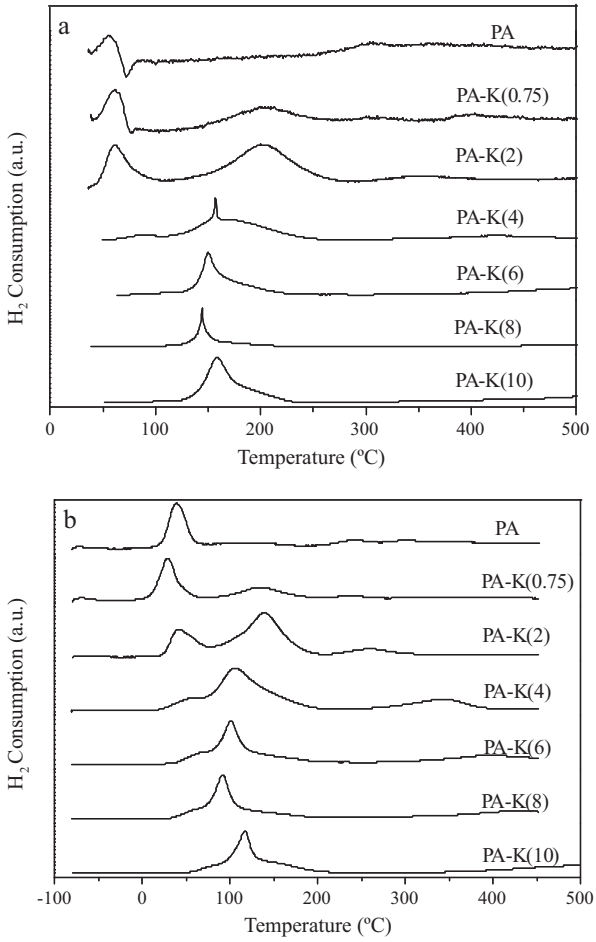

Fig. 3. H_2-TPR profiles of the investigated catalysts: (a) start at ambient temperature and (b) start at −80 °C.

quite sharp and intense. (3) The change in intensity is accompanied by a general downward shift of all the bands: for example, band I undergoes a shift from the value 2083 cm^{-1} in PA to 2063 cm^{-1} in PA–K(8%) which is taken at peak, whereas band III undergoes a

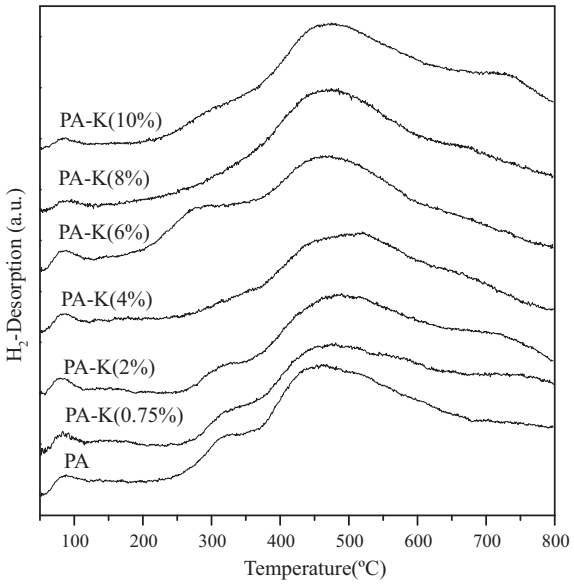

Fig. 4. H_2-TPD profiles on reduced catalysts.

downward shift of −116 cm^{-1} (from 1940 cm^{-1} in PA to 1824 cm^{-1} in PA–K(8%), value taken at peak). The phenomenon shows that the doping of K results in a red shift of the ν(CO) stretching frequency of species adsorbed on these sites, which implies strengthening of the Pd–CO bond with the increase of K content.

3.1.5. Furfural-TPSR

Programmed thermodesorption of furfural and the decarbonylation products was done to verify the stability of surface species occurring during desorption and decomposition on PA and PA–K catalysts. These experiments were performed with the adsorption of furfural/He flow on reduced catalysts at 40 °C for 1.5 h, then purging the physisorption of furfural, after that, monitoring the desorbing products with the online MS. Masses characteristic of different desorption products are shown in Fig. 6, including furfural ($C_5H_4O_2$, 96 amu), furan (C_4H_4O, 68 amu), carbon monoxide (CO, 28 amu) and hydrogen (H_2, 2 amu).

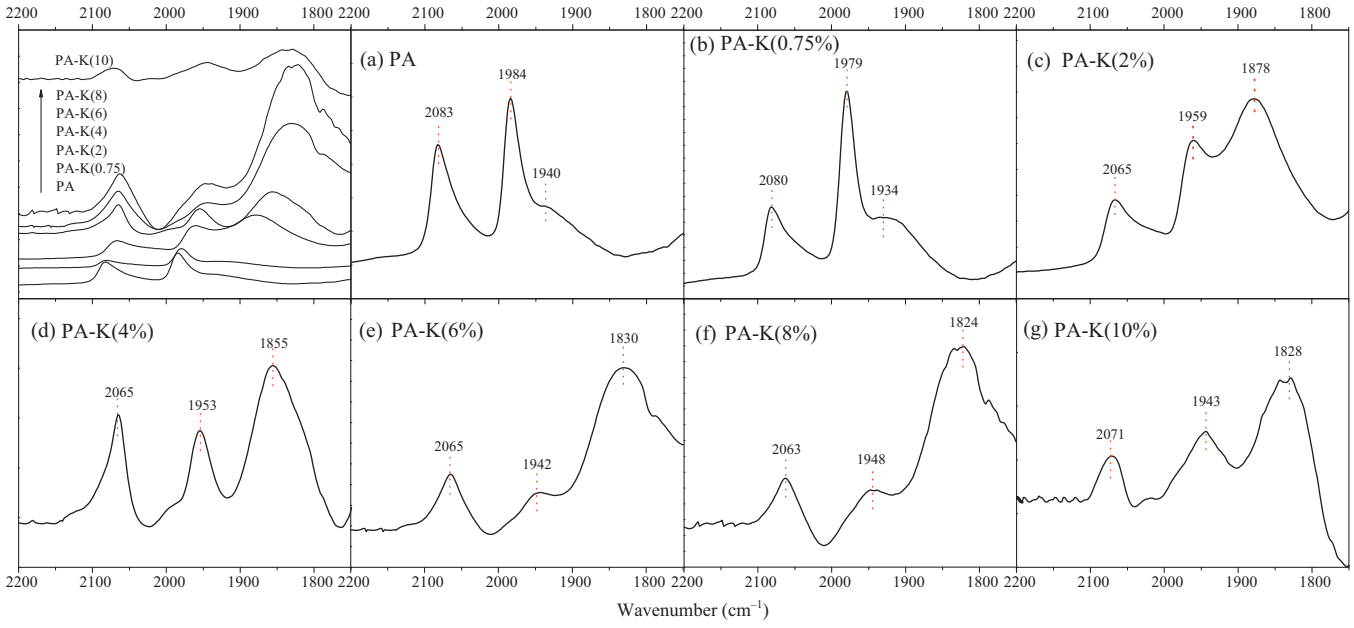

Fig. 5. FTIR spectra of CO dosed at 20 °C on the catalysts.

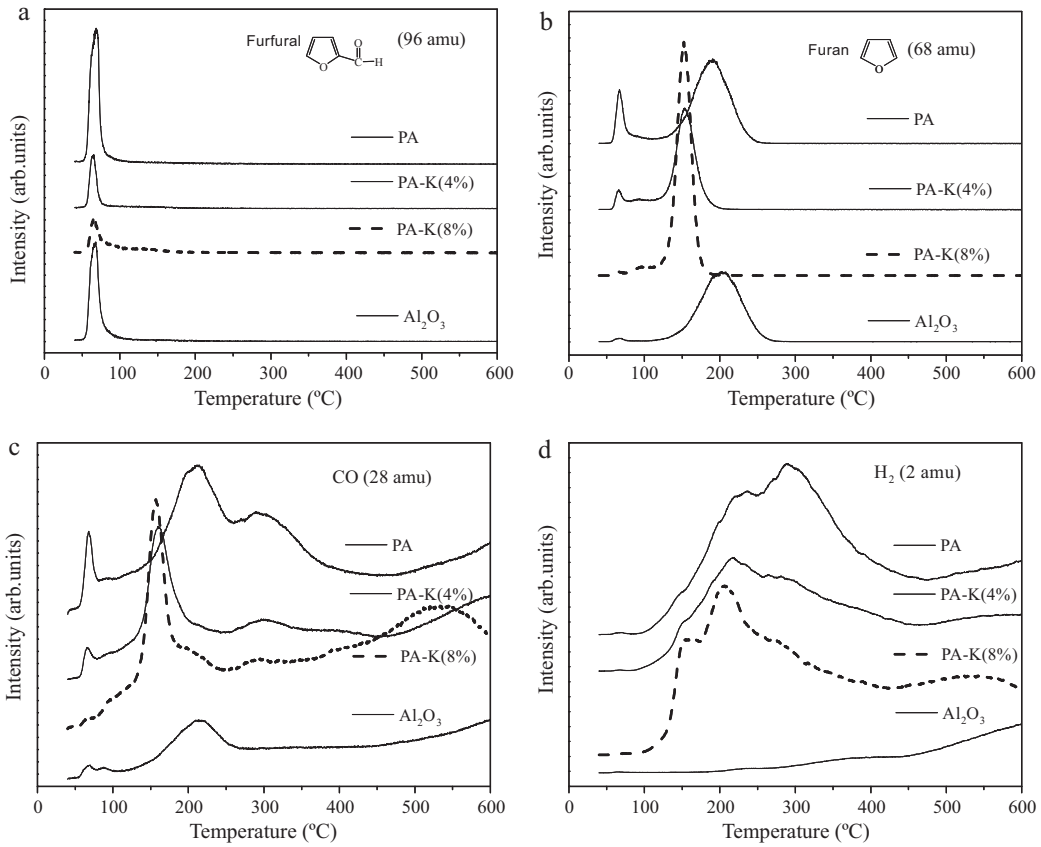

Fig. 6. Furfural-TPSR on the catalysts: (a) furfural desorption, (b) furan desorption, (c) CO desorption, and (d) H_2 desorption.

Fig. 6a shows that furfural desorption takes place at ca. 67 °C, and the intensity of furfural desorption peak is decreased with the increase of K content, which may be due to the strong adsorption between furfural and Pd in the presence of K. Also, the support can adsorb a certain amount of furfural, with its intensity higher than PA–K and lower than PA catalyst, indicating that the adsorbability of furfural on Al_2O_3 is weak and the adsorption quantity is small.

Fig. 6b and c expresses the desorption peaks of furan and CO (the products of furfural decarbonylation), respectively. In Fig. 6b, two desorption peaks of furan are presented in PA catalyst: a small peak at ca. 67 °C and a large peak at ca. 195 °C. In comparison, the PA–K(4%, 8%) catalysts also have two desorption peaks: the low temperature peaks are decreased of the intensity, but keeping the same temperature as PA; the high temperature peaks are at ca. 152 °C, which is 43 °C lower than that of PA catalyst, implying that furan can be easier desorbed on PA–K catalysts than on PA catalyst. It is interesting to see that the support also presents two desorption peaks of furan at 66 °C and 208 °C. However, the result of blank test shows that the decarbonylation reaction cannot occur on the support (Al_2O_3). Fig. 6c also exhibits that the desorption quantity of CO on Al_2O_3 is obviously less than other Pd-containing catalysts. Furthermore, the first two desorption peaks of CO on these catalysts exhibit the similar desorption temperature as furan desorption, in other words, furan desorption is accompanied by desorption of CO. The CO desorption peaks on PA appear at 68, 214 and 290 °C, while the peaks on PA–K are at 68, 158 and 290 °C. The third desorption peak (290 °C) may be due to the strong interaction between Pd and CO, which is decreased with the increase of K content. However, an additional desorption peak of CO on PA–K (8%) is present at ca. 530 °C, which may be due to the decomposition of polymer.

Fig. 6d displays the H_2 desorption from the investigated catalysts. In this characterization, the samples were purged with He at 350 °C before the absorption of furfural, so the desorbed hydrogen was mainly coming from furfural. As shown in the figure, H_2 is desorbed more easily from PA–K catalysts than from PA catalyst. In addition, it is obvious that there are no sign of H_2 desorption on Al_2O_3, which suggests that the desorbed hydrogen is formed in the presence of Pd. During the process of reduction, H_2 can be adsorbed dissociatively on the Pd surface and further spill to the support. As revealed by H_2-TPD, the spillover hydrogen is hardly desorbed completely lower than 350 °C (Fig. 4). Therefore, the first desorption peak may be due to the hydrogen atoms released to the surface by the decomposition of the furfural adlayer recombined and desorbed, while the second desorption peak may be due to the combination of two hydrogen atoms derived from dehydrogenation of furfural and spillover hydrogen, respectively.

3.1.6. *Furfural-FTIR*

To better understand the promoter effects on the decarbonylation reaction, we investigated the interaction of reduced PA and PA–K(8%) with furfural. The in situ FTIR spectra of furfural adsorbed at different temperature on the samples are displayed in Fig. 7.

Fig. 7a shows the adsorbed acyl species of furfural on PA catalyst. At 30 °C, two bands observed at 1888 cm^{-1} and 1695 cm^{-1} can be attributed to physisorbed and chemisorbed furfural, which are similar to the adsorption of benzaldehyde on Pd/Al_2O_3 [23]. With increasing the temperature, the physisorbed furfural is decreased the intensity and the bands shift to lower frequency, while the chemisorbed furfural only decreases the intensity. In addition, a new band appeared at 80 °C (1957 cm^{-1}), which is assigned to the CO adsorption, is progressive increased the intensity with further increase the temperature. It indicates that the increase of temperature promotes the decarbonylation of furfural.

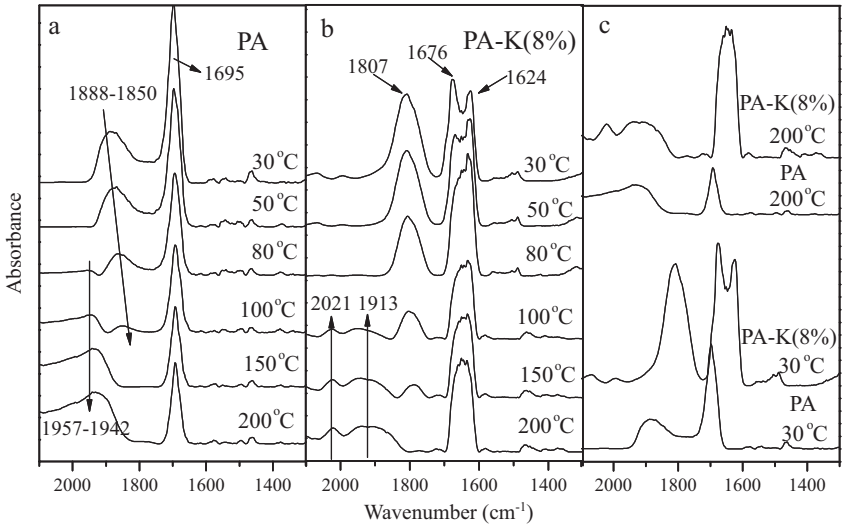

Fig. 7. In situ FTIR of furfural adsorbed on the catalysts at different temperature: (a) adsorbed on PA catalyst, (b) adsorbed on PA–K(8%) catalyst, and (c) comparison of K-doped and undoped catalysts.

Fig. 7b exhibits the adsorbed acyl species of furfural on PA–K(8%) catalyst. The band at 1807 cm^{-1} is attributed to the physisorbed furfural, which is also decreased the intensity with increasing the temperature. It is interesting to see that the chemisorbed furfural on the K-doped catalyst shows two bands at 1676 cm^{-1} and 1624 cm^{-1}, suggesting the presence of two different adsorbed modes. With increasing the temperature, the band at 1676 cm^{-1} is decreased the intensity, which is the same as the change of adsorbed furfural at 1695 cm^{-1} on PA catalyst (Fig. 7A). However, the band at 1624 cm^{-1} has no significant change. Furthermore, the CO bands can be seen at 1913 cm^{-1} and 2021 cm^{-1} at the temperature higher than 100 °C.

As indicated in Fig. 7c, the differences of furfural in situ IR spectra on the K-doped and undoped samples can be summarized in three main phenomena. (1) The intensity of furfural adsorption bands (both physisorbed and chemisorbed furfural) on PA–K(8%) are higher than that on PA, which indicates that the adsorption of furfural is stronger on K-doped samples. (2) The PA–K(8%) catalyst shows a conspicuous shift of all furfural adsorption bands to lower frequency compared with PA. For example, the chemisorbed band undergoes a shift from the value 1695 cm^{-1} in PA to 1676 cm^{-1} in PA–K(8%). (3) In contrast to PA, the PA–K(8%) displays two chemisorbed bands: the first band is at 1676 cm^{-1}, having the same adsorption mode with band 1695 cm^{-1} on PA; and the "new band" is at 1624 cm^{-1}, which is gradually dominant with increasing the temperature. Accordingly, the doping of K can change the adsorption mode of furfural on Pd catalysts, which has promoting effect on the catalytic performance.

3.2. Catalytic performance

Sample catalysts were tested for furfural decarbonylation to examine the effect of added different K sources and different K content on the performance of Pd/Al_2O_3 (PA) catalyst. The results are plotted in Figs. 8 and 9, which have four small graphs represented as furfural conversion, furan selectivity, furan and tetrahydrofuran yield, 2-methylfuran selectivity, respectively. Again, we emphasize that the focus of our research is to improve the yield of furan and tetrahydrofuran at low temperature (below 300 °C), as well as minimize 2-methylfuran selectivity.

Fig. 8 shows the results of conversions, selectivities and yields about the catalytic tests, and it can be clearly seen that PA catalyst reveal a maximum for furfural conversion and in contrast, lowest furan selectivity and highest 2-methylfuran selectivity. In comparison with PA catalyst, the conversions of furfural on the K-doped catalysts are all decreased to a certain extent, whereas the furan selectivities are all increased (Fig. 8a and b). In other words, the doping of K can suppress the hydrogenation of furfural and promote the decarbonylation reaction on Pd catalyst. Fig. 8c exhibits that the total yield of furan and tetrahydrofuran does not all increase with K doping, for example, PA–KCl catalyst shows the lowest yield, which may be due to the residual presence of chlorine poisoned the active sites. The total yields of furan and tetrahydrofuran on the K-doping catalysts with different K salts follow the order of $PA–K_2CO_3 > PA–KOH > PA > PA–KNO_3 > PA–KAc > PA–KCl$. The last graph (Fig. 8d) shows that PA–KCl, PA–KAc and $PA–K_2CO_3$ catalysts have excellent behavior on suppressing hydrogenation of furfural to 2-methylfuran. Therefore, considering the yield of furan and 2-methylfuran selectivity, K_2CO_3 as K precursor can obtain the best catalyst performance in the decarbonylation reaction.

Next, the experiments of the decarbonylation reaction were carried out on different content of K (from K_2CO_3), and the results can be seen from Fig. 9. The first graph (Fig. 9a) shows that the catalyst PA–K(6%) has the highest furfural conversion, which is not the expected result that the furfural conversion is decreased with the increase of K content. H_2-TPD (Fig. 4) shows that the PA–K(6%) has the largest amount of hydrogen desorption below 300 °C followed by PA–K(4%), PA–K(2%) and PA–K(8%), which is coincident with the furfural conversion. It is revealed that the decrease of desorbed hydrogen would decrease the hydrogenation activity, which is eventually decreased the furfural conversion. However, the opposite trend is observed for furan selectivity (Fig. 9b). PA–K(8%) exhibits the highest furan selectivity, while PA–K(0.75%) shows the lowest. As shown in Fig. 9c, PA–K(8%) displays the highest yield of furan (99.5%), while PA–K(0.75%) and PA–K(10%) exhibit lower yields than other catalysts above 220 °C. It is also noticed that the selectivity of 2-methylfuran is zero when the loading of K is above 4% (Fig. 9d).

4. Discussion

Furfural is an unsaturated aldehyde of five carbons, which is readily hydrogenated under hydrogen atmosphere. Generally, thermodynamic studies favor hydrogenation of C=C bond over the C=O bond for hydrogenation reaction of unsaturated aldehydes [24,25]. Reaction kinetics also prefer hydrogenation of the C=C bond over C=O bond for small molecules, whereas steric constraints

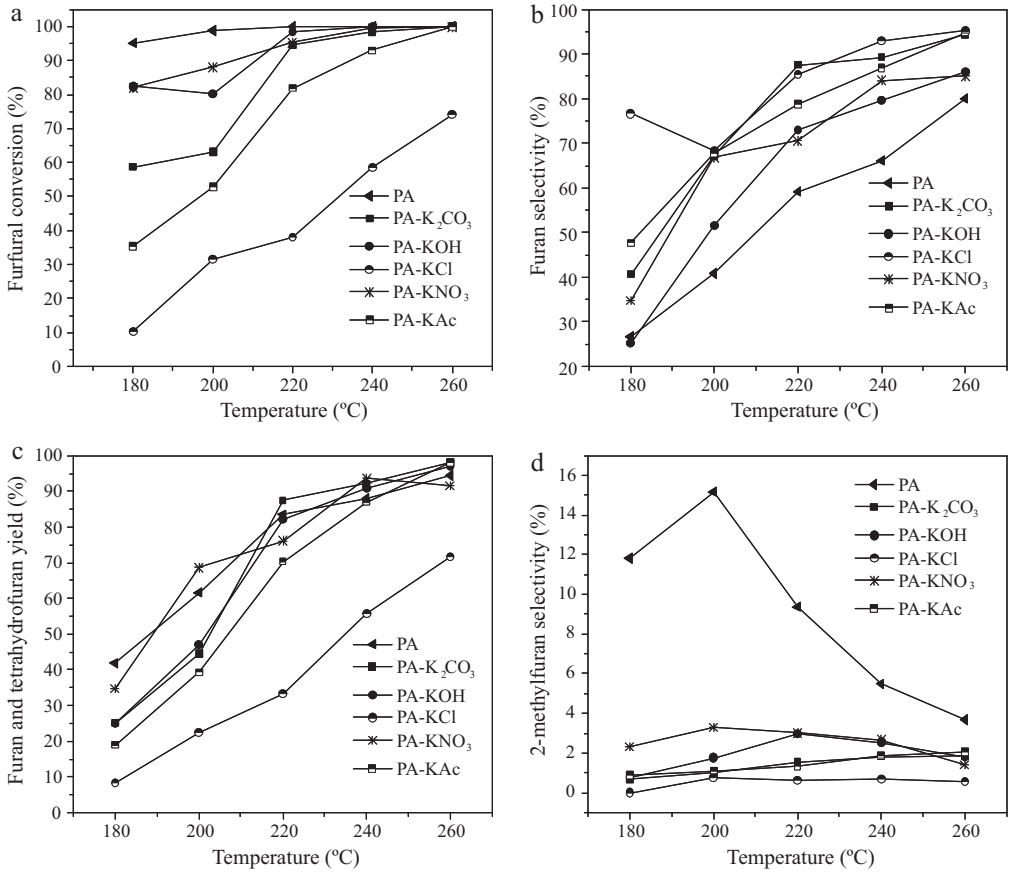

Fig. 8. Catalytic activity of Pd–K catalysts with doping different K salts in decarbonylation of furfural: (a) conversion of furfural, (b) selectivity of furan, (c) total yield of furan and tetrahydrofuran, and (d) selectivity of 2-methylfuran. Reaction conditions: atmospheric pressure, WHSV = 0.77 h^{-1}, H_2/furfural = 20 (molar ratio).

for larger molecules decrease the rates for hydrogenation of C=C bond. Accordingly, the hydrogenation of C=C bond in furfural is more difficult than that of C=O bond, which may be due to the steric effects or the aromatic character of furfural. In our work, however, the hydrogenation of furfural should be decreased as much as possible, especially for the C=O bond hydrogenation. It has been reported that Pd exhibits a low rate for hydrogenation the C=O bond compared with other metals commonly used for hydrogenation [26]. In addition, the catalytic performance shows that a clear and positive effect for the suppressing hydrogenation of furfural is present by doping of K. The role of K in the suppressing hydrogenation on the Pd catalysts can be better interpreted taking into account the interaction between Pd particles and the dopant. Usually, alkali metals are employed as catalytic promoters or modifiers to increase the activity and lifetime of heterogeneous catalysts, but the role played by alkali metals is not unequivocal, depending on the type of solid and catalytic reaction. Firstly, alkali oxides can neutralize the surface acidic sites, thus enhancing their resistance to poisoning by acid. Furthermore, many studies [27,28] suggest that the alkali metal atoms modify the local electron density of the transition metal either directly or through the support, which can be approved by XPS. However, the alkali metals are always introduced as oxides, hydroxides, carbonates and nitrates. Thus, it is explained that K strongly segregates at the surface, forming a submonolayer of adsorbed K and O having a stoichiometric ratio of unity.

4.1. Characters and activity effect of K on Pd catalysts

The catalyst evaluation results exhibit that the doping of K on Pd catalysts can enhance the decarbonylation of furfural to furan and simultaneously decrease the selectivity of hydrogenation by-products, especially 2-methylfuran.

According to the BET results of PA–X catalysts, the PA–KAc catalyst exhibits the highest surface area but shows less active in furfural decarbonylation compared with other catalysts except PA–KCl (Fig. 8a). A reversed trend is observed for PA–KNO_3 samples with lower surface area and higher catalytic activity. Besides, with the increase of K content (using K_2CO_3 as the K precursor), the surface area and pore volume are decreased monotonous, whereas the conversion of furfural does not follow the same order. Therefore, the catalytic activity should depend on other factors, rather than the specific surface area. Fig. 10 shows that large amounts of crystalline alkali carbonate are deposited on the surface, but the promoter phase is always an alkali compound other than carbonate [29]. In other words, the promoter phase is part of dispersed K in some chemical state, which may be formed through the interaction between K and the activity species.

H_2-TPR shows that the addition of K changes the reduction profile of PA catalyst, favoring the reduction at higher temperatures. It also indicates that the high temperature reduction peak is attributed to the interaction between K and Pd^{2+}. When the K content is over 4%, the high temperature peak is dominated, and shifts to lower temperature with further increase of K content. Besides, the decrease of low temperature peak proves that "free Pd atoms" (do not interact with K) are decreased with increasing K content. When the K content is higher than 4%, the "free Pd atoms" are almost disappeared, which presents the same trend as the selectivity of 2-methylfuran. In other words, the selectivity of 2-methylfuran is decreased with the decrease of "free Pd atoms" and is approach to zero at the K content of 4 wt.%. For the PA–K(10%), the reduction

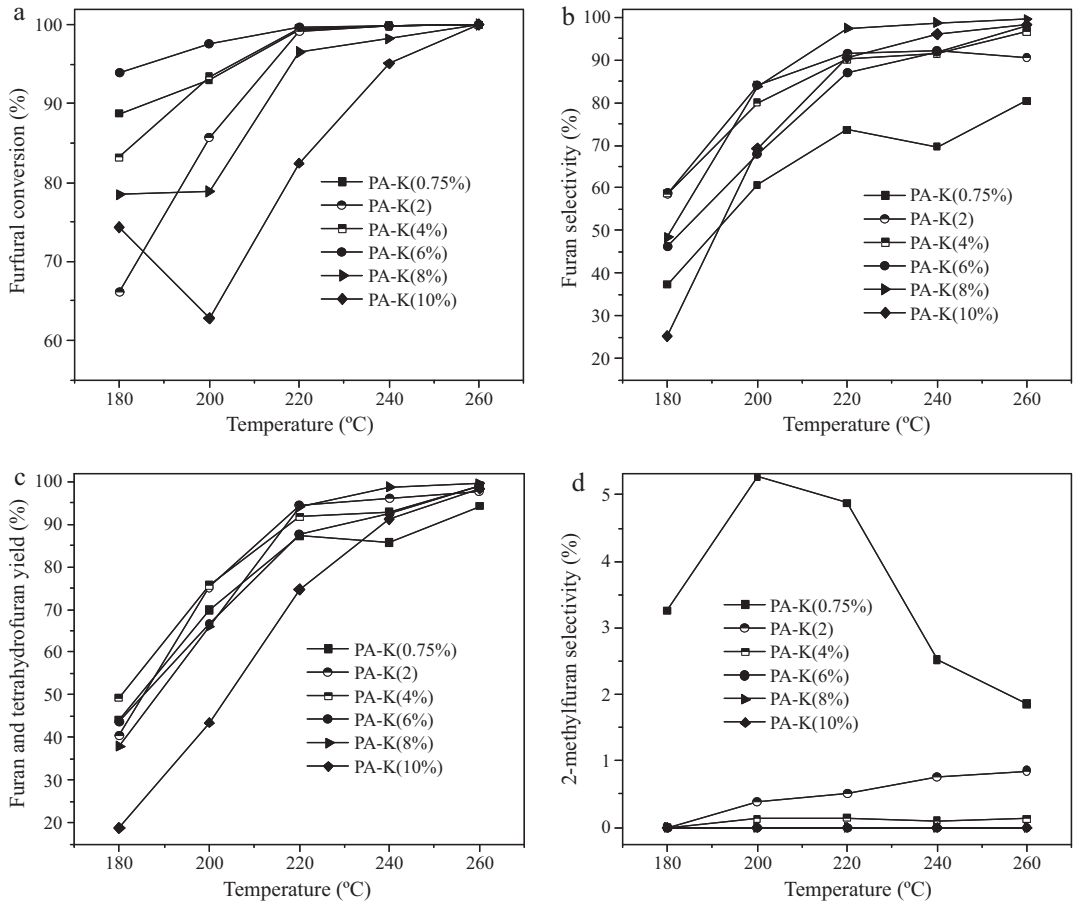

Fig. 9. Catalytic activity of Pd–K catalysts with doping different K content in decarbonylation of furfural: (a) conversion of furfural, (b) selectivity of furan, (c) total yield of furan and tetrahydrofuran, and (d) selectivity of 2-methylfuran. Reaction conditions: atmospheric pressure, WHSV = 0.77 h^{-1}, H_2/furfural = 20 (molar ratio).

peak shifts to high temperature compared with PA–K(8%), and the activity is obviously decreased. One reason might be that the active sites are blocked by carbonate, and another reason might be that the promoting effect is suppressed by some poisoning function of the higher alkali content [30].

The modification induced by alkali addition on metal adsorption properties has been widely reported in the literature. Kiskinova studying hydrogen adsorption on alkali modified nickel indicated that these additives give rise to an important decrease in hydrogen dissociation ability and saturation coverage [31]. Weatherbee indicates that K produced an increase in the activation energy for hydrogen adsorption on K promoted Fe/SiO_2 catalyst [32]. Praliaud reported that K caused a decrease of the hydrogen adsorption, explained this by a decrease in metallic phase accessibility or by a rise of hydrogen bond stoichiometry, and claimed this occurrence induced by an alkali "sieving effect" that limits the accessibility of the metal surface to a larger probe molecules [33]. The H_2-TPD results (Fig. 4) show that the doping of K can suppress the spillover hydrogen and H_2 may interact with the alkali-modified support, in other words, interact with hydroxyl groups on support. Therefore, K-doping acts to enhance the adsorption strength of hydrogen, and this effect should tend to reduce the rate of hydrogenation reaction, either by increase the hydrogenation-reaction activation energy, decreasing the concentration of "free" H_a [34]. Besides, increasing of K content induces different behavior towards the adsorption of CO on Pd particles and the CO-FTIR spectra show that the intensity is increased and accompanied by a general red-shift of all the bands. The sample PA–K(8%) shows the strongest interaction with CO and the main CO absorption band is isolated bridged carbonyls. Also, the PA–K(8%) exhibits the best performance on furfural decarbonylation, which may be owing to the adsorption mode and the strong interaction between furfural and the catalyst.

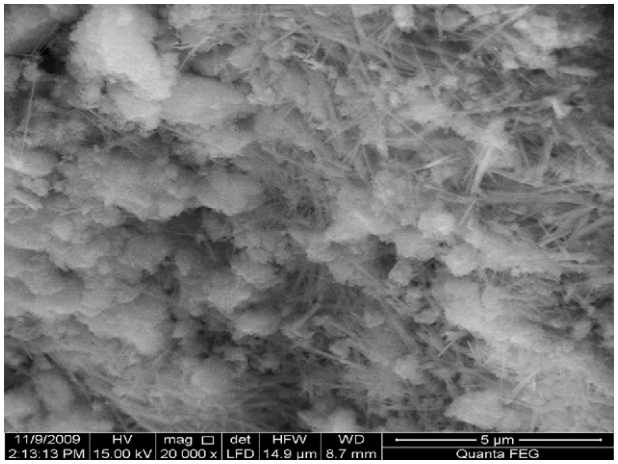

Fig. 10. SEM images of the surface of Pd–K(8%)/Al_2O_3 particles (5 μm).

4.2. Electronic effect of K on Pd catalysts

As indicated by the results of H_2-TPR, a mixed compound (KPdO) may be formed through the strong chemical interaction between K^+ and Pd^{2+} species, which is more difficult to reduce than PdO. With the increase of K content (from 2% to 8%), the mixed com-

pound is more likely to be reduced and the reason might be that increasing of K content can share more electrons with Pd^{2+} during the process of reduction. Due to the higher electronegative of Pd atom, an electronic density transfer is readily from alkali metal to Pd, which is proved by XPS with a shift towards negative values of the Pd 3d binding energies [35]. Also, alkali adsorbates also cause a dramatic enhancement of the electronic polarizability of the metal surface extending it several angstroms into the vacuum [36]. This effect also produces a general shift towards lower frequencies of the CO bands as indicated by the CO-FTIR spectra on these catalysts, owing to an enhanced transfer of electron density from the metal to the π^* molecular orbitals of CO.

Electronic effects of K promoter on Pd can take place either through direct K–Pd interaction or through a modification of the support properties which induces a change in metal–support interactions. The addition of K_2CO_3 can make the support properties change from acidic to basic [37] and the electron transfer between metals and supports has been suggested by several researchers [38,39]. Figoli and L'argeniere studied the selective hydrogenation of styrene over Pd/Al_2O_3 catalysts and discovered the changes in the electronic state of Pd via XPS when sodium was added to the support. Free electrons on Pd were transferred to lower electron density sites on acidic Al_2O_3 and electron transfer was attenuated with added sodium [38]. Figueras et al. studied benzene hydrogenation over Pd supported on several different acidic oxides and claimed that the support influences the electronic properties of Pd [39]. In our work, more basic nature of K-doped Al_2O_3 favors an electron transfer to Pd, resulting in a higher Pd electron density, and ultimately a reduced strength of hydrocarbon adsorption on Pd. This interaction leads to an increase in furan selectivity from furfural because the furan desorbs more readily before it can be further hydrogenated to tetrahydrofuran, and simultaneously results in a decrease of the furfural hydrogenation by-products.

4.3. Adsorption mode of furfural on PA and PA-K catalysts

The results of CO-FTIR indicate that the doping of K can transfer electronic density to Pd and change the adsorption mode of CO. During the decarbonylation reaction, the surface of Pd displays negative charge in the presence of K, while the adsorbed furfural simultaneously dehydrogenates and then forms carbonyl C^+ ions. As a result, the adsorption of furfural is stronger on PA–K than that of PA catalyst, which can be proved by the results of furfural-FTIR (Fig. 7) and is in agreement with the results that the intensity of furfural desorption peaks are decreased with the increase of K content (Fig. 6a). Also, the strong binding between furfural and PA–K can promote the cleavage of C–C, that is to say the strong adsorption facilitates the furfural decarbonylation, as indicated by the furan desorption (Fig. 6b). Barteau have studied the adsorption mode of aldehydes on Pd(1 1 1) and Pd(1 1 0) surfaces by a combination of TPD and HREELS, mainly for adsorption in the low temperature regime[40,41]. At lower temperatures aldehydes tend to bond in the η_1(O) configuration (that is, adsorb on the metal surface through the oxygen lone pair electrons), a weakly held form which desorbs at low temperatures, typically ca. 200 K. A more strongly bonded η_2(C,O) configuration (π-bonded through carbon and oxygen and flat-lying) is identified above 200 K, and it appears that decomposition or decarbonylation occurs through this state [42]. However, Barteau proposed that the decarbonylation process of aldehydes is carried out through the state of η_1(C) on Pd(110), which is transformed from η_2(C,O) [43].

On the basis of furfural-TPSR and furfural-FTIR studies, the following bond activation sequence is proposed to occur during furfural decarbonylation on Pd catalysts (Fig. 11). Firstly, furfural adsorption in the η_1(O) configuration is not stable under our operational temperature and can be transformed easily to η_2(C,O) configuration [40]. Then, a small part of furfural decarbonylates through this adsorption mode [42] (Fig. 11a) which is labeled as η_2(C,O)-furfural. Accordingly, the decarbonylation product furan can be obtained at ca. 67 °C, which is observed as the first furan desorption peak occurred both on PA and PA–K catalysts (Fig. 6b). Secondly, the lone-pair electrons of carbonyl oxygen displays negative charge and the surface of Pd also exhibits a negative electric field induced by K, so the adsorption of carbonyl oxygen is more difficult on PA–K than on PA. As a result, the amount of η_2(C,O)-furfural will be decreased by K doping, which suggests that the furan produced through η_2(C,O)-furfural will be decreased with the increase of K content. As shown in Fig. 6b, it is obvious that the intensity of the first furan desorption peaks is decreased accompanied by increasing K content. Furthermore, the hydrogenation of furfural always occurs through η_2(C,O) configuration, that is the C=O bond hydrogenation [23], so the decrease of η_2(C,O)-furfural caused by K doping will inhibit the hydrogenation reaction. For PA catalyst, the main decarbonylation occurs through η_1(C) configuration (Fig. 11b), which is transformed from η_2(C,O) configuration [43]. However, for PA–K catalysts, the results of furfural-FTIR (Fig. 7) show that the adsorption mode of acyl species is different on K-doped and undoped catalysts, and furfural-TPSR indicates that the η_2(C,O) configuration is difficult to form and unstable on PA–K catalysts. Accordingly, the main decarbonylation of furfural on the K-doped samples may occur through η_1'(C) configuration (Fig. 11c), which is more stable than η_1(C) configuration.

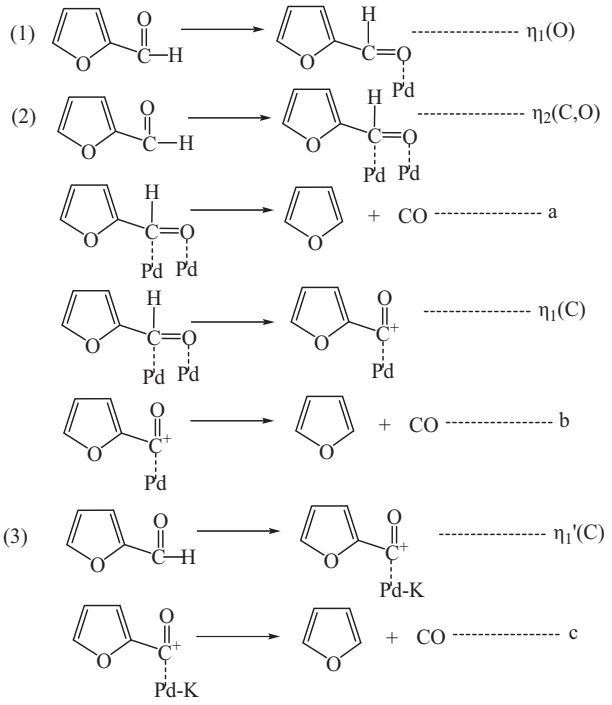

Fig. 11. Adsorption mode of furfural on Pd/Al_2O_3 and $Pd–K/Al_2O_3$ catalysts.

5. Conclusions

In this work, the catalytic behaviors of K-doped Pd/Al_2O_3 catalysts for furfural decarbonylation have been investigated in the temperature range of 180–260 °C and ambient pressure. According to the results, the $Pd–K/Al_2O_3$ catalyst doped with K_2CO_3 and with a K-loading of 8 wt.% shows the best performance in the decarbonylation reaction (the conversion of furfural is 100% and the yield of furan is 99.5% at 260 °C). Besides, the selectivity of 2-methylfuran will approach zero when the loading of K is above 4 wt.%. The effect

of K is systematically investigated through several characterization methods, which can be summarized as follows: (1) K doping has a great influence on Pd^{2+} precursor phase and the reduced Pd atom. TPR data indicates that there exists a strong interaction between K and Pd^{2+}, which inhibits the reduction of Pd^{2+} species. The results of CO-FTIR and H_2 chemisorption also suggest that the strong interaction still exists between K and the reduced Pd atoms. (2) K doping has caused the red-shift of CO adsorption, which suggests that more basic nature of K-doped Al_2O_3 results in an electron transfer to Pd, leading to a higher Pd electron density, and ultimately promoting the decarbonylation of furfural. (3) The furfural-TPSR and furfural-FTIR results indicate that the doping of K can change the adsorption mode of furfural on Pd catalysts. Finally, it is important to mention that the decrease of η_2(C,O) configuration might be the main reason for suppressing hydrogenation of furfural on K-doped Pd catalysts.

Acknowledgement

The authors gratefully thank the financial supports of Natural Science Foundation of China (No. 20976185).

References

[1] A. Corma, S. lborra, A. Velty, Chem. Rev. 107 (2007) 2411–2502.
[2] K.J. Zeitsch, The Chemistry and Technology of Furfural and Its Many By-products, vol. 13, 1st ed., Elsevier, Amsterdam, 2000.
[3] H. Singh, M. Prasad, R.D. Srivastaval, J. Chem. Technol. Biotechnol. 30 (1980) 293–296.
[4] J. Coca, E.S. Morrondo, J.B. Parra, H. Sastre, React. Kinet. Catal. Lett. 20 (1982) 3–4.
[5] K.J. Jung, A. Gaset, Biomass 16 (1988) 63–76.
[6] P.A. Moshkin, E.A. Preobrazhenskaya, B.B. Berezina, V.E. Markovich, E.G. Kudrina, V.P. Papsueva, E.A. Sokolina, Khimiya Oeterotsiklicheskikh Soedinenii. 2 (1966) 3–7.
[7] J. Coca, E.S. Morrondo, H. Sastre, J. Chem. Technol. Biotechnol. 32 (1982) 904–908.
[8] G.M. Whitman, US 2,374,149 (1945).
[9] D.G. Manly, J.P. O'Halloran, US 3,223,714 (1965).
[10] P. Lejemble, A. Gaset, Philippe Kalck, Biomass 4 (1984) 263–274.
[11] A.P. Dunlop, G.W. Huffman, US 3,257,417 (1966).
[12] K.J. Jung, A. Gaset, Biomass 16 (1988) 89–96.
[13] R.D. Srivastava, A.K. Guha, J. Catal. 91 (1985) 254–262.
[14] Y. Yang, H.W. Xiang, Y.Y. Xu, L. Bai, Y.W. Li, Appl. Catal. A 266 (2004) 181–194.
[15] R. Pellegrini, G. Leofanti, G. Agostini, L. Bertinetti, S. Bertarione, E. Groppo, A. Zecchina, C. Lamberti, J. Catal. 267 (2009) 40–49.
[16] G. Neri, G. Rizzo, L. De Luca, A. Donato, M.G. Musolino, R. Pietropaolo, Appl. Catal. A 356 (2009) 113–120.
[17] A.H. Padmasri, A. Venugopal, J. Krishnamurthy, K.S. Rama Rao, P. Kanta Rao, J. Mol. Catal. A 181 (2002) 73–80.
[18] P. Paraskevi, I.K. Dimitris, J. Catal. 267 (2009) 57–66.
[19] A.A. Davydov, Infrared Spectroscopy of Adsorbed Species on the Surface of Transition Metal Oxides, Wiley, New York, 1990.
[20] X.Z. Jiang, Y.H. Sua, B.J. Lee, S.H. Chien, Appl. Catal. A 211 (2001) 47–51.
[21] W.J. Kim, J.H. Kang, I.Y. Ahn, S.H. Moon, Appl. Catal. A 268 (2004) 77–82.
[22] S. Bertarione, D. Scarano, A. Zecchina, V. Johanek, J. Hoffmann, S. Schauermann, M.M. Frank, J. Libuda, G. Rupprechter, H.J. Freund, J. Phys. Chem. B 108 (2004) 3603.
[23] C. Keresszegi, D. Ferri, T. Mallat, A. Baiker, J. Catal. 234 (2005) 64–75.
[24] B.B. Baeza, I.R. Ramos, A.G. Ruiz, Appl. Catal. A 205 (2001) 227–237.
[25] R. Zanella, C. Louis, S. Giorgio, R. Touroude, J. Catal. 223 (2004) 328–339.
[26] T.B.L.W. Marinelli, S. nabuurs, V. ponec, J. Catal. 151 (1995) 431–438.
[27] A. Daz, D.R. Acosta, J.A. Odriozola, M. Montes, J. Phys. Chem. B 101 (1997) 1782–1790.
[28] W.D. Mross, Catal. Rev. 25 (4) (1983) 591–637.
[29] A.J. Urquhart, J.M. Keel, F.J. Williams, R.M. Lambert, J. Phys. Chem. B 107 (2003) 10591–10597.
[30] C.P. Huang, J.T. Richardson, J. Catal. 51 (1978) 1–8.
[31] M.P. Kiskinova, Studies in Surface Science and Catalysis, vol. 70, 1992, 149.
[32] G.D. Weatherbee, J.L. Rankin, C.H. Bartholimew, Appl. Catal. 11 (1984) 73.
[33] H. Praliaud, M. Primet, G.A. Matin, Appl. Surf. Sci. 17 (1983) 107.
[34] J.W. Federico, P. Alejandra, T. Samuel, S.T. Mintcho, M.L. Richard, J. Phys. Chem. B 106 (2002) 5668–5672.
[35] F.L. Leonarda, A.M. Guy, G.D. Giulio, J. Catal. 164 (1996) 322–333.
[36] S. Stolbov, T.S. Rahman, Phys. Rev. Lett. 96 (2006) 186801–186804.
[37] H.P. Yeung, L.P. Geoffrey, Ind. Eng. Chem. Res. 31 (1992) 2.
[38] N.S. Figoli, P.C. L'argeniere, Catal. Today 5 (1989) 403.
[39] F. Figueras, R. Gomez, M. Primet, Adu. Chem. Ser. 121 (1973) 480.
[40] M. Mavrikakis, M.A. Barteau, J. Mol. Catal. A 131 (1998) 135.
[41] J.L. Davis, M.A. Barteau, J. Am. Chem. Soc. 111 (1989) 1782–1792.
[42] M. Bowker, R. Holroyd, N. Perkins, J. Bhantoo, J. Counsell, A. Carley, C. Morgan, Surf. Sci. 601 (2007) 3651–3660.
[43] R. Shekhar, M.A. Barteau, R.V. Plank, J.M. Vohs, J. Phys. Chem. B 101 (1997) 7939–7951.